A Comparison of Reconstruction Methods for Compressed Sensing of the Photoplethysmogram

Nicholas J. Conn
Microsystems Engineering
Rochester Institute of Technology
Rochester, New York 14623
Email: nicholasjconn@ieee.org

David A. Borkholder, PhD
Microsystems Engineering
Rochester Institute of Technology
Rochester, New York 14623
Email: david.borkholder@rit.edu

***Abstract*—Compressed sensing has the possibility to significantly decrease the power consumption of wireless medical devices. The photoplethysmogram (PPG) is a device which can greatly benefit from compressed sensing due to the large amount of power needed to capture data. The aim of this paper is to determine if the least absolute shrinkage and selection operator (LASSO) optimization algorithm is the best approach for reconstructing a compressively sampled PPG across varying physiological states. The results show that LASSO reconstruction approaches, but does not surpass, the reliability of constrained optimization.**

I. Introduction

Compressed sensing is the process of sampling a sparse signal at a rate significantly lower the Nyquist rate [1]. The Nyquist rate is defined as twice the highest frequency of the measured signal. Compressed sensing involves reconstructing a sample vector of length N from a set of M random measurements, where M is much less than N. These M measurements are captured using a randomly generated sensing matrix, which is used to reconstruct the sample vector by estimating the coefficients in sparse domain of the signal being measured.

In 2006, the seminal papers on compressed sensing were published by Candes and Donoho [2]–[5]. These papers discuss the mathematical principles behind compressed sensing. They have shown that a signal has a very high probability of being exactly reconstructed when the signal has a known sparse domain and is measured using a sensing matrix that is incoherent to the basis functions of the signal's sparse domain.

Previous work has shown the success of the least absolute shrinkage and selection operator (LASSO) optimization algorithm for reconstruction of compressively sensed physiological signals [6]. More specifically, the work from Beheti introduces the use of a weighted LASSO technique for reconstructing a compressively sensed photoplethysmogram (PPG), but does not compare it to constrained ℓ_1 norm reconstruction [7], [8].

LASSO allows for a balance between minimizing the norm of the sparse domain and maintaining measurement accuracy by adhering to the constraints imposed by the measurement vector. This trade-off is determined by the LASSO penalty parameter, which is a constant that must be chosen before implementation [9]. For this reason, LASSO is a popular reconstruction method for the compressed sensing of signals which contain measurement noise.

The PPG is used in many medical devices to attain blood oxygenation levels, heart rate, and other cardiac intervals. To estimate the blood oxygenation level (SpO2), the ratio between the root mean square (RMS) of PPG signals captured at two separate wavelengths can be used [8]. This paper quantitatively shows how different LASSO penalty parameters affect important aspects of the PPG such as the root mean square (RMS) and temporal information change when compared to constrained optimization. The purpose of this paper is to determine if LASSO provides any benefit over constrained optimization for reconstructing the PPG across a range of physiological states.

Section II includes a mathematical introduction to compressed sensing, an explanation of different reconstruction methods, and the metrics used for determining the accuracy of reconstruction. In Section III, results are presented and analyzed. Finally, Section IV provides a short summary and concluding remarks.

II. Theory

A. Overview of Compressed Sensing

Compressed sensing is the process of utilizing only M measurements to reconstruct a discrete signal of length N, where $M \ll N$. The level of compression achieved can be represented by the under sampling ratio (USR), which is N divided by M. For compressed sensing to work, the sample vector $\vec{\mathbf{x}}$ must be sparse in some domain [10]. By multiplying $\vec{\mathbf{x}}$ by the discrete cosine matrix $\mathbf{\Psi}$, the PPG is shown to be sparse in the discrete cosine domain (Fig. 1). This process is shown in (1).

$$\mathbf{\Psi} \cdot \vec{\mathbf{x}} = \vec{\mathbf{s}} \tag{1}$$

Given that $\vec{\mathbf{x}} \in \mathbb{R}^N$ is sparse it is multiplied by a sensing matrix, $\mathbf{A} \in \mathbb{R}^{M \times N}$. This results in the measurement vector $\vec{\mathbf{y}} \in \mathbb{R}^M$, as shown in (2).

$$\mathbf{A} \cdot \vec{\mathbf{x}} = \vec{\mathbf{y}} \tag{2}$$

The only requirement for the sensing matrix is that it is incoherent to the basis functions of the sparse domain, $\mathbf{\Psi}$. Normally, this is achievable by populating $\mathbf{A}$ with values generated from a random distribution [10]. The sensing matrix

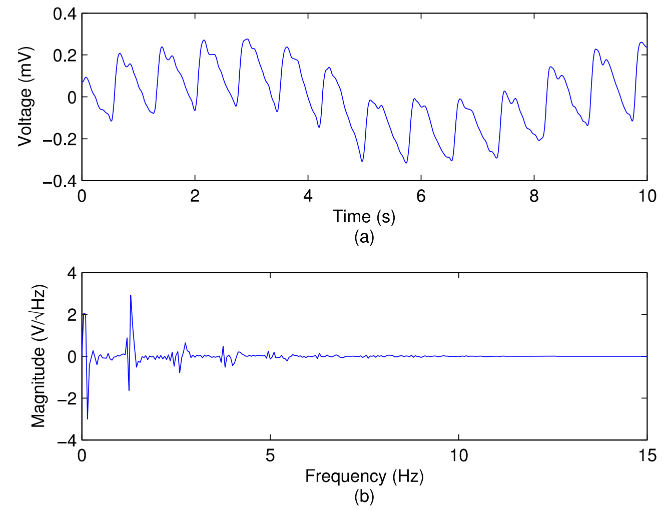

Fig. 1. The sparsity of a 10 second (N = 1600) long PPG signal (a) is shown in the discrete cosine domain (b).

used in this research is generated using an identity matrix, which is an orthogonal set of impulse functions. The process used for this is shown in (3), where random rows are removed from an identity matrix to create $\mathbf{A}$. This structure was chosen so that not all samples in $\vec{\mathbf{x}}$ are used to generate $\vec{\mathbf{y}}$.

$$\mathbf{A} = \begin{bmatrix} 1 & 0 & 0 & 0 & 0 & 0 \\ 0 & 1 & 0 & 0 & 0 & 0 \\ 0 & 0 & 1 & 0 & 0 & 0 \\ 0 & 0 & 0 & 1 & 0 & 0 \\ 0 & 0 & 0 & 0 & 1 & 0 \\ 0 & 0 & 0 & 0 & 0 & 1 \end{bmatrix} = \begin{bmatrix} 1 & 0 & 0 & 0 & 0 & 0 \\ 0 & 0 & 0 & 1 & 0 & 0 \\ 0 & 0 & 0 & 0 & 0 & 1 \end{bmatrix} \quad (3)$$

The process shown in (2), which uses both $\mathbf{A}$ and $\vec{\mathbf{x}}$ to generate $\vec{\mathbf{y}}$, forms an under-determined linear system which is used as constraints during reconstruction.

B. Reconstruction

Typically, the reconstruction process for compressed sensing can be defined as a convex optimization problem [2], [10]. Given the under-determined linear system in (2) and the matrix transform that projects $\vec{\mathbf{x}}$ onto a sparse basis shown in (1), the optimization problem is defined as

$$\min_{\hat{\mathbf{x}} \in \mathbb{R}^N} \|\mathbf{\Psi} \cdot \hat{\mathbf{x}}\|_1 \text{ subject to } \vec{\mathbf{y}} = \mathbf{A} \cdot \hat{\mathbf{x}} \ . \quad (4)$$

This will minimize the ℓ_1 norm of the sparse coefficients, while exactly adhering to constraints imposed by the measurement vector and sensing matrix. This method, also called constrained optimization, typically does not perform well when in applications where measurement noise is present [9], [10].

One method for accurately reconstructing a signal in the presence of noise is least absolute shrinkage and selection operator (LASSO) based optimization, shown in (5) [6]. By adjusting the penalty parameter λ, the amount of deviation from (2) can be specified, allowing for a more robust overall reconstruction for signals that contain noise [6], [9].

$$\min_{\hat{\mathbf{x}} \in \mathbb{R}^N} \{\lambda \|\mathbf{\Psi} \cdot \hat{\mathbf{x}}\|_1 + \|\vec{\mathbf{y}} - \mathbf{A} \cdot \hat{\mathbf{x}}\|_2^2\} \quad (5)$$

This approach can be expanded further by incorporating a weighting vector for the sparse domain. The weighting vector is generated using *a priori* information and can greatly increase the accuracy of the reconstructed waveform. This method can be used on any signal that has a typical or characteristic set of coefficients in its sparse domain.

The results in this paper use the discrete cosine domain as the sparse domain of the PPG. The weighting vector $\vec{\mathbf{w}}$ for the sparse domain used is generated in (6) from the average sparse domain coefficients for the signal being captured. The average sparse domain $\bar{\mathbf{s}}$ can be found by averaging a set of training signals together.

The larger the weighting coefficient, the smaller the reconstructed sparse domain coefficient will be. The maximum possible value of $\vec{\mathbf{w}}$ is determined by σ, a small constant. When the average sparse coefficient is zero, the maximum weighting is $1/\sigma$. By integrating the weighting vector into constrained ℓ_1 norm optimization, (7) is defined.

$$[w]_i = \frac{1}{[\bar{s}]_i + \sigma} \qquad i = 0, 1, \cdots, N-1 \quad (6)$$

$$\min_{\hat{\mathbf{x}} \in \mathbb{R}^N} \| \langle \vec{\mathbf{w}}, (\mathbf{\Psi} \cdot \hat{\mathbf{x}}) \rangle \|_1 \text{ subject to } \vec{\mathbf{y}} = \mathbf{A} \cdot \hat{\mathbf{x}} \quad (7)$$

Similarly, a weighted LASSO minimization is formed in (8).

$$\min_{\hat{\mathbf{x}} \in \mathbb{R}^N} \{\lambda \| \langle \vec{\mathbf{w}}, (\mathbf{\Psi} \cdot \hat{\mathbf{x}}) \rangle \|_1 + \|\vec{\mathbf{y}} - \mathbf{A} \cdot \hat{\mathbf{x}}\|_2^2\} \quad (8)$$

The results presented in Section III use the weighting vector shown in (6) for both LASSO based reconstruction and constrained ℓ_1 norm optimization.

C. Error Metrics

Two very important measurements which can be extracted from the PPG are the blood oxygenation level (SpO2), and when used in conjunction with a synchronized ECG, the pulse transit time. For this reason, two different metrics are used to compare the accuracy of the reconstructed sample vector to the original Nyquist sample vector, the change in RMS and the change in the location of the PPG foot.

In order to show how reconstruction errors affect the estimated SpO2 levels, the percent change in RMS value is used. This percentage is determined by normalizing the change in RMS to the original signal's RMS value, as shown in (9).

$$RMS_{diff} = \frac{|RMS(\vec{\mathbf{x}}) - RMS(\hat{\mathbf{x}})|}{RMS(\vec{\mathbf{x}})} \quad (9)$$

Even small errors in the reconstructed frequency domain can result in peak deformation and other temporal changes that will not be apparent when only using (9). In fact, maintaining

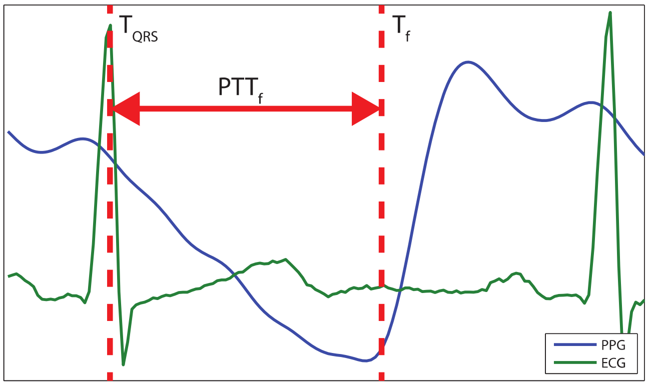

Fig. 2. By locating the foot of the PTT (T_f) and the QRS peak on the ECG (T_{QRS}), the pulse transit time (PTT_f) can be found.

the temporal accuracy of physiological signals is required for many applications.

An important temporal feature of the PPG is the location of the foot in each beat. By determining the interval between the ECG QRS peak and the PPG foot, the pulse transit time (PTT) can be estimated. Fig. 2 illustrates how the PTT is estimated for a given beat and (10) shows how the normalized PTT is calculated. A signal's PTT is calculated by averaging the PTT for each beat. It is important to note that the ECG was not compressively sampled since it is used as a baseline to determine how specific locations of the reconstruction differs from the original signal.

$$PTT_f = \frac{|(T_f - T_{QRS}) - (\widehat{T}_f - T_{QRS})|}{T_f - T_{QRS}} \quad (10)$$

Finally, in order to show how the penalty parameter affects the time of reconstruction, the time it took to reconstruct 60 seconds of data was captured directly in MATLAB.

III. Results and Discussion

The physiological data sets used were attained under informed consent in a protocol approved by the Rochester Institute of Technology Institutional Review Board for Protection of Human Subjects. The Biopac MP36 (Biopack Systems, Inc., Goleta, CA) was used to capture synchronized ECG and ear PPG at a sample rate of 50 kHz.

One minute measurements were captured at eleven different activity levels to test how well each reconstruction method performs across a range of physiological states. Before each measurement was analyzed, it was decimated to a sample rate of 160 Hz to more closely match the Nyquist sampling rate found in physical systems. Each minute sample was split into five sample vectors with an N of 1920 (a window size of 12 seconds) for compressed sensing.

To further increase the reliability of the results provided, each metric is averaged across eleven activity levels and four different random sensing matrices generated using (3). The following tests were performed in MATLAB (R2012a) using CVX, a package for specifying and solving convex optimization problems [11], [12].

The results in Fig. 3 show that larger penalty parameters correspond to a higher RMS error for a wide range of USRs. A more detailed look at how the penalty parameter affects the RMS accuracy for a specific USR is shown in Fig. 4. This more clearly shows how different LASSO penalty parameters perform when compared to the constrained ℓ_1 norm reconstruction shown in (4).

When using constrained ℓ_1 norm reconstruction, the average RMS percent difference is 8% with a standard deviation of 1.7%. For penalty parameters below 0.003, the RMS percent difference is less than 10% with an average standard deviation of approximately 2.1%.

As discussed in Section II, analyzing the temporal accuracy of a reconstructed physiological signal is very important. For a USR of 16, the PTT foot error results are shown in Fig. 5 and show a higher error rate than the percent RMS difference; this is due to the fact that the algorithm used to detect the foot of the PPG is not perfectly robust in the presence of noise.

As the penalty parameter decreases, the standard deviation and error rate approach that of the constrained ℓ_1 norm reconstruction. This is the same trend shown in the RMS error

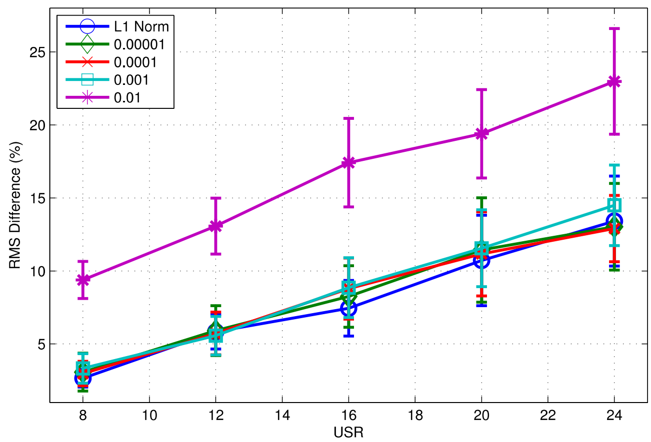

Fig. 3. The difference in RMS for different LASSO penalty parameters decreases as the penalty parameter decreases.

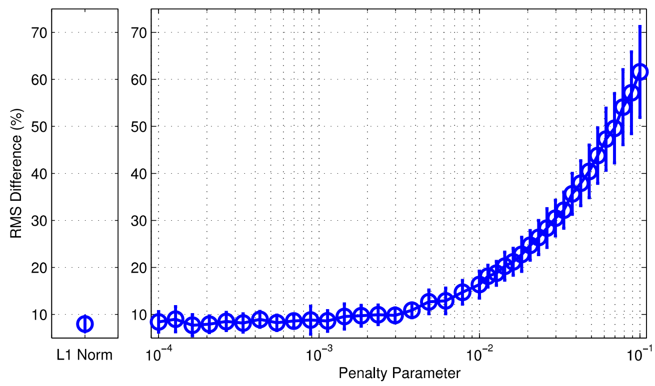

Fig. 4. As the penalty parameters decreases at a USR of 16, the RMS difference approaches the rate and variance of the constrained ℓ_1 norm error (on the left).

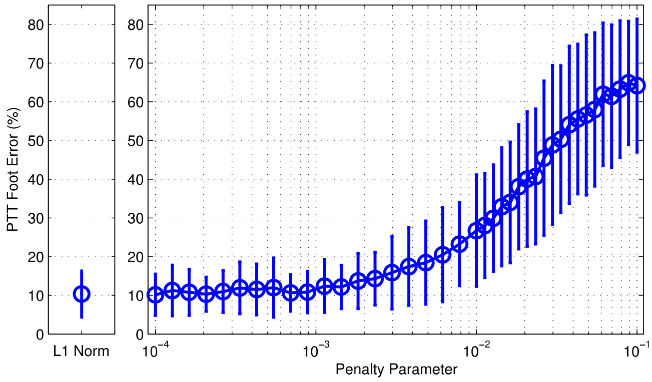

Fig. 5. While the standard deviation of the PTT_f is higher than that of the RMS difference, the general trend is the same at a USR of 16. As the penalty parameter decreases, the accuracy increases.

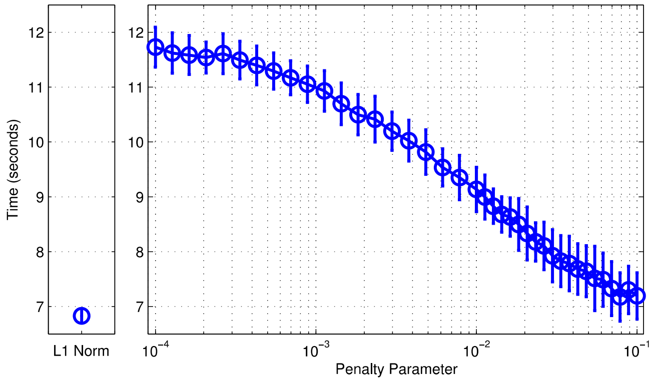

Fig. 6. Lower penalty parameters correspond to significantly higher reconstruction times when compared to constrained ℓ_1 norm reconstruction at a USR of 16.

results. For penalty parameters below 0.001 the average error rate is 11% with a standard deviation of 6%. While the smaller penalty parameters perform just as well as the ℓ_1 norm method for both of these metrics, they do not perform any better. The ℓ_1 norm method has an error rate of 10.35% with a standard deviation of 6%.

Finally, the average reconstruction time for different penalty parameters for a USR of 16 and a window size of 12 seconds is shown in Fig. 6. As the penalty parameter becomes smaller, the reconstruction time increases. While the overall increase in reconstruction time is small, approximately 5 seconds, it can become significant for larger window sizes.

When noise distorts the measurement vector $\vec{\mathbf{y}}$ in (2), LASSO typically allows for a decrease in reconstruction variability compared to constrained ℓ_1 norm reconstruction [5], [9], [10]. The results presented herein utilize low noise physiologic signals, which may explain why LASSO based reconstruction performs as well, but not better than, ℓ_1 norm reconstruction.

IV. Conclusion

These results shown that a compressively sampled PPG can be accurately reconstructed using both weighted LASSO reconstruction and weighted constrained ℓ_1 norm reconstruction across a range of physiological states (activity levels). Based on a Nyquist sample rate of 160 Hz, compressed sensing of the PPG can be achieved with a USR of 16 while maintaining an overall error rate of approximately 10%, this corresponds to an average sample rate of 10 Hz.

LASSO based reconstruction with penalty parameters below 0.001, is just as reliable and accurate as constrained ℓ_1 norm reconstruction. Given that it is also slower than the constrained ℓ_1 norm reconstruction, LASSO offers no quantitative befit for the compressed sensing of the PPG.

Future research should compare LASSO based reconstruction to constrained ℓ_1 norm reconstruction, on a physical compressed sensing system, by measuring and reconstructing physiological signals which contain noise that distort the measurement vector. Additionally, the affect different sparse domains have on the accuracy of reconstruction for the PPG should be investigated.

Acknowledgment

The authors would like to thank Jeff Lillie and Cody Cziesler for their technical support and for gathering the subject data used for this publication. They would also like to thank National Semiconductor for their support.

References

[1] A. V. Oppenheim, R. W. Schafer, and J. R. Buck, *Discrete-time signal processing (2nd ed.)*. Upper Saddle River, NJ, USA: Prentice-Hall, Inc., 1999.
[2] D. Donoho, “Compressed sensing,” *Information Theory, IEEE Transactions on*, vol. 52, no. 4, pp. 1289 –1306, april 2006.
[3] D. Donoho and Y. Tsaig, “Recent advances in sparsity-driven signal recovery,” in *Acoustics, Speech, and Signal Processing, 2005. Proceedings. (ICASSP ’05). IEEE International Conference on*, vol. 5, march 2005, pp. v/713 – v/716 Vol. 5.
[4] E. Candes and T. Tao, “Near-optimal signal recovery from random projections: Universal encoding strategies?” *Information Theory, IEEE Transactions on*, vol. 52, no. 12, pp. 5406 –5425, dec. 2006.
[5] E. J. Candes, J. K. Romberg, and T. Tao, “Stable signal recovery from incomplete and inaccurate measurements,” *Communications on Pure and Applied Mathematics*, vol. 59, no. 8, pp. 1207–1223, 2006. [Online]. Available: http://dx.doi.org/10.1002/cpa.20124
[6] A. Dixon, E. Allstot, A. Chen, D. Gangopadhyay, and D. Allstot, “Compressed sensing reconstruction: Comparative study with applications to ecg bio-signals,” in *Circuits and Systems (ISCAS), 2011 IEEE International Symposium on*, may 2011, pp. 805 –808.
[7] P. Baheti and H. Garudadri, “An ultra low power pulse oximeter sensor based on compressed sensing,” in *Wearable and Implantable Body Sensor Networks, 2009. BSN 2009. Sixth International Workshop on*, june 2009, pp. 144 –148.
[8] P. K. Baheti, H. Garudadri, and S. Majumdar, “Blood oxygen estimation from compressively sensed photoplethysmograph,” in *Wireless Health 2010*, ser. WH ’10. New York, NY, USA: ACM, 2010, pp. 10–14. [Online]. Available: http://doi.acm.org/10.1145/1921081.1921084
[9] D. Angelosante, G. Giannakis, and E. Grossi, “Compressed sensing of time-varying signals,” in *Digital Signal Processing, 2009 16th International Conference on*, july 2009, pp. 1 –8.
[10] E. Candes and M. Wakin, “An introduction to compressive sampling,” *Signal Processing Magazine, IEEE*, vol. 25, no. 2, pp. 21 –30, march 2008.
[11] CVX Research, Inc., “CVX: Matlab software for disciplined convex programming, version 2.0 beta,” http://cvxr.com/cvx, Sep. 2012.
[12] M. Grant and S. Boyd, “Graph implementations for nonsmooth convex programs,” in *Recent Advances in Learning and Control*, ser. Lecture Notes in Control and Information Sciences, V. Blondel, S. Boyd, and H. Kimura, Eds. Springer-Verlag Limited, 2008, pp. 95–110, http://stanford.edu/~boyd/graph_dcp.html.